Hidden safety in structural design codes

Max Teichgräber Jochen Köhler Daniel Straub

January 27, 2022

Abstract: Structural design codes are deliberately kept simple in order to limit the complexity of the design process. To ensure sufficient safety with simplified models, parameters of these models are often chosen conservatively. This leads to additional "hidden safety" in the design. But what happens if one utilizes more advanced design models without the implicit conservatism of the simple models? On one hand, an advanced design method has the potential to result in more optimized designs. On the other hand, it will affect the structural safety. While the advanced models might be associated with smaller uncertainty, which increases reliability, the loss of hidden safety can decrease the reliability. We comprehensively discuss the role of hidden safety in codified structural design and its effects on the reliability and material consumption. Based on this, we develop a framework for adapting the safety concept to ensure that advanced models lead to the same level of safety as standard models. The framework is exemplarily applied to the wind load model of the Eurocode.

1. Introduction

Structural design codes aim to provide easy-to-use rules that lead to economical and safe structures [1]. They are the result of a long evolutionary process, which began with the construction of buildings based on a “trial and error” approach, intuition, and experiments on scale models [2]. In the 18th century, a fundamental shift took place: The design of structures was increasingly based on physical models and theories [3–6]. Engineers had tools to predict the load bearing capacity of structures with confidence and had to rely less on experience. In order to standardize the process and address the variability and uncertainty in loads and materials, structural design codes were developed from the late 19th century onward. These codes were based on the global safety factor concept.

Today’s structural design codes are based mainly on the semi-probabilistic partial safety factor (PSF) concept, which was introduced in the late 1970s [7–11]. This is based on utilizing multiple PSFs for different actions and resistances, which are multiplied with their corresponding characteristic values. In contrast to the use of a single global safety factor, the semi-probabilistic concept can better address the specific uncertainties associated with a specific design situation and thus lead to a more homogeneous safety level. For this reason, it is considered an adequate trade-off between ease-of-use and optimality of the resulting design [12].

The PSFs and characteristic values prescribed in current design codes are obtained through a code calibration process [13–15]. PSFs that lead to design reliabilities that are as close as possible to the target reliability in a large number of design situations are identified [16]. As discussed in [12], target reliabilities are based on previous codes and regulations, which reflect the legacy experience. This backward calibration ensures that a new code does not lead to drastic changes of the safety level. Past code calibrations also ensure that the resulting designs of specific structures do not vary significantly between subsequent code generations.

Design codes are based on the use of models that approximate the real loads and structural responses. The parameters of these models, the values of which are often prescribed by the codes, also evolved from experience. In many instances, these parameter values were selected conservatively (i.e., they lead – on average – to an underestimation of resistances and an overestimation of actions). These conservative choices introduce a *hidden safety* into the design.

The effect of this hidden safety is difficult to quantify, and it has not been considered explicitly in past code calibration. This had not been an issue in the past because of the calibration of PSFs to previous codes: As long as models covered by the new code and the corresponding parameter choices remained the same as in the old code, the backward calibration ensured that the overall level of safety remained approximately the same.

However, hidden safety can lead to problems when new models are applied. Advances in computational structural analysis, data collection, and enhanced data-driven modeling can make the use of advanced modeling techniques feasible. Examples include computational fluid dynamics (e.g., virtual wind tunnel tests) [17], seismic analysis (e.g., earthquake simulations) [18], collection of on site data (e.g., wind velocity measurements or geotechnical test), or tests on scale models (e.g., physical wind tunnel tests or geotechnical centrifuge modeling). In general, the use of these modeling techniques is desirable in view of more economic and sustainable structures. However, the hidden safety associated with existing models can be lost when using them. It is therefore imperative that the effects of hidden safety be quantified.

While most experts are aware of this hidden safety challenge, it has not received much attention in the scientific literature. Only a small number of publications explicitly mention the challenges related to hidden safety. These include Byfield and Nethercot [19], who examined various constructional steelwork resistance models (e.g., the bending resistance of restrained beams or the shear-buckling resistance of plate girders) and adapted the respective PSFs in order to homogenize the safety level. Holicky et al. [20] investigated the influence of different probabilistic models (distribution choices and distribution fitting techniques) of the time variant and time invariant wind load model components to the probability of failure. Nowak et al. [21] calculated the probability of failure of bridges and compared it to the probability of failure including measurements of inner forces. Gomes and Beck [22] proposed a conservatism index to classify structural models. Other publications involving hidden safety include Toft et al. [23], Hanninen et al. [24], and Gazetas et al. [25]. However, none of these publications provides a general framework on how to consider hidden safety in the PSF concept.

In this paper, we provide a framework on how to quantify the effects of hidden safety on the reliability and the design. We utilize this framework to describe how the PSF concept can be adapted if standard models – which potentially include hidden safety – are replaced by more advanced models. The framework is exemplarily applied to the wind load model of the Eurocode, which is compared with more advanced wind load modeling techniques.

2. Partial safety factor concept

According to the PSF concept [7–11], a structural design must fulfill the following inequality throughout the structure:

$$e_d \leq r_d \tag{1}$$

where

$$e_d = \gamma_F \cdot e_k \tag{2}$$

$$r_d = \frac{r_k}{\gamma_M} \tag{3}$$

Here e_k and r_k are the characteristic values of action effects and resistances, e_d and r_d the corresponding design values, and γ_F and γ_M the PSFs of action effects and resistances. Characteristic values are usually defined as quantile values of the probability distributions, i.e., as lower quantile values on the resistance side and higher quantile values on the load side.

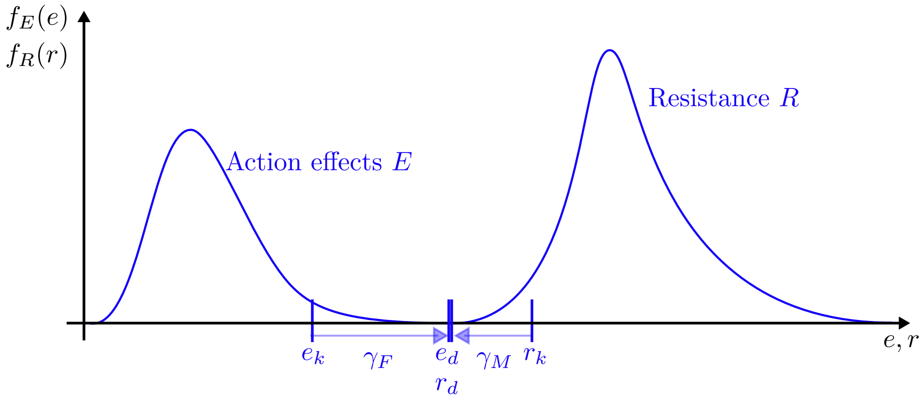

Figure 1: Basic reliability problem.

The choice of the two safety components – the PSFs and the characteristic values – is based on reliability analysis. Figure 1 illustrates the probabilistic view of the action effects E and the resistance R. Based on these, a limit state function $g(R, E) = R - E$ can be defined to estimate the probability of failure $\Pr(F)$ as the integral of the joint probability density function (PDF) $f_{R,E}(r,e)$ over the failure domain $\Omega_F = \{r,e \mid g(r,e) < 0\}$:

$$\Pr(F) = \int_{\Omega_F} f_{R,E}(r, e)\, \mathrm{d}r\, \mathrm{d}e \tag{4}$$

Using the inverse of the standard normal cumulative distribution function (CDF) Φ^{-1}, a reliability index β can be calculated as:

$$\beta = -\Phi^{-1}(\Pr(F)) \tag{5}$$

Characteristic values and the PSFs can be calibrated such that a target reliability index is achieved. Under the assumption that the current reliability is satisfactory and accepted by society, the target reliability index is typically chosen as the average reliability index of the status quo [15, 26, 27]. The calibration thus maintains the reliability level. The current reliability level may not be ideal; however, a modification of the reliability level should be conducted in its own separate calibration procedure.

In addition to the two well-known explicit safety components, namely the choice of the

PSFs and the characteristic values, there is a third, often overlooked, implicit safety component: the hidden safety. Hidden safety arises if models are conservative, i.e., they overestimate the loads and their effects or underestimate the resistances. [1]

Hidden safety is considered implicitly in the choice of PSFs and characteristic values. This is because these values are historically and iteratively adapted on the basis of structures built by these models. As long as the same models are used, investigations about hidden safety are not required. But what happens if the standard models are replaced by a more advanced and presumably more accurate models? This replacement affects the reliability of structures in two counteracting ways:

- More advanced models usually have less model uncertainty. This increases the reliability of a structure that complies with inequality (1).

- The loss of conservativeness leads to an on average lower design resistance. This reduces the structural reliability.

Depending on which of these effects dominates, the structural reliability can either increase or decrease. In order to preserve the same level of safety, an explicit treatment of hidden safety is needed. The goal of this paper is to investigate and formalize hidden safety and show how it can be addressed in the PSF concept.

[1] A precondition for hidden safety is model based design; hence, hidden safety is a consequence of the fundamental shift of the 18th century from experience-based to model-based design. The application of engineering models has a trade-off: On one hand, an engineer gets an insight and a better understanding of nature and therefore is able to predict the structural behaviors. On the other hand, the applied models are only approximations of reality, and their predictions contain an error. This error is not explicitly included in the PSF concept.

3. Hidden safety

In this section, we provide a detailed description of hidden safety and quantify its effects on structural design and reliability. At the end of the section, we show how the elimination of hidden safety can be compensated by modifying PSFs or utilizing adjusted characteristic values.

Since hidden safety has not been discussed much in the scientific literature, we provide a detailed description of (effects of) hidden safety in the following, which is kept as universal as possible. A compact step by step guidance on the implementation of advanced models in the PSF concept is given in Section 3.6.

3.1. Definitions

Hidden safety is closely related to the accuracy of the models used in structural design as well as its effect on the structural design and structural reliability. In this context, we define some essential terms. We make a distinction between aleatoric and epistemic uncertainty. Following [28], we consider as *aleatoric* the uncertainty that cannot be eliminated within the confines of the current state of science. In contrast, *epistemic uncertainty* is due to limited knowledge. Epistemic uncertainty can be reduced by collecting information (e.g., through tests or improved models).

On this basis, we define the following terms:

- *Aleatoric distribution*, is the probability distribution that includes only aleatoric uncertainty.

- *Aleatoric probability of failure* is calculated with the aleatoric distributions.

- *Nominal probability of failure* is calculated considering both, aleatoric and epistemic uncertainties.

Although the definition of aleatoric and epistemic uncertainty is not very precise and arguable, it is sufficient in this context. Detailed and philosophically well-founded discussions can be found in [29–36].

3.2. Hidden safety in structural codes

We investigate hidden safety in the context of the PSF concept. We use the terminology of Eurocode; however, the conclusions are equally valid for other design codes.

In a Eurocode design, four different models can identified (Figure 2): The load model $\mathcal{M}_{L,EC}$, the structural model $\mathcal{M}_{S,EC}$, the material model $\mathcal{M}_{M,EC}$, and the resistance model $\mathcal{M}_{R,EC}$. We use the subscript EC to stress that these models are provided by the Eurocode.

$$
\begin{array}{lcl}
\text{Load model } \mathcal{M}_{L,EC} & & \text{Material model } \mathcal{M}_{M,EC} \\
\downarrow & & \downarrow \\
\text{Characteristic load } l_{k,EC} & & \text{Characteristic material } m_{k,EC} \\
\downarrow & & \downarrow \\
\text{Partial safety factor } \gamma_f & & \text{Partial safety factor } \gamma_m \\
\downarrow & & \downarrow \\
\text{Structural model } \mathcal{M}_{S,EC} & & \text{Resistance model } \mathcal{M}_{R,EC} \\
\downarrow & & \downarrow \\
\text{Partial safety factor } \gamma_{Sd} & & \text{Partial safety factor } \gamma_{Rd} \\
\downarrow & & \downarrow \\
\text{Design load effect } e_{d,EC} & \overset{!}{\geqslant} & \text{Design resistance } r_{d,EC}
\end{array}
$$

Figure 2: Overview of the Eurocode design approach.

$\mathcal{M}_{L,EC}$ and $\mathcal{M}_{M,EC}$ are typically statistics-based models, which provide distributions for the load L_{EC} and the material property M_{EC}. In the PSF concept, these distributions are represented by characteristic values. Moreover, the design load effect and the design resistance are calculated via functions $t_{S,EC}$ and $t_{R,EC}$ provided by the structural model

$\mathcal{M}_{S,EC}$ and the resistance model $\mathcal{M}_{R,EC}$. The four PSFs γ_f, γ_{Sd}, γ_m and γ_{Rd} address the uncertainty of the load model, the structural model, the material model and the resistance model.

Remark: For the sake of simplicity, the Eurocode merges the PSFs of the action and the resistance side

$$\gamma_F = \gamma_f \times \gamma_{Sd} \tag{6}$$

$$\gamma_M = \gamma_m \times \gamma_{Rd} \tag{7}$$

To improve understanding we stick with the separated notation. Moreover, some codes use the global safety factor format (e.g. the reinforced concrete structures [37]). This case is also covered as it is a special case of the partial safety factor format.

Considering all models explicitly, Equations 2 and 3 can be reformulated to Equation 8 and 9 and Figure 1 can be extended to Figure 3:

$$e_d = \gamma_{Sd} \cdot t_{S,EC} \left(\gamma_f \cdot l_{k,EC} \left(L_{EC}\right)\right) \tag{8}$$

$$r_d = \frac{1}{\gamma_{Rd}} \cdot t_{R,EC} \left(\frac{m_{k,EC}(M_{EC})}{\gamma_m}\right) \tag{9}$$

Eurocode defines only the characteristic values of the load and the material properties explicitly and not the corresponding PDFs $f_{L_{EC}}$ and $f_{M_{EC}}$. As a consequence, $f_{E_{EC}}$ and $f_{R_{EC}}$ are also not explicitly defined. These distributions can be implicitly inferred from background documentations (e.g., [38–40]) and from the distributions used in the calibration of the Eurocode safety components (e.g., [16]).

As previously discussed, hidden safety is a result of conservative models for structural design. For establishing what a conservative design is, we refer to the design one would obtain based on aleatoric distributions in combination with the PSFs and the definition

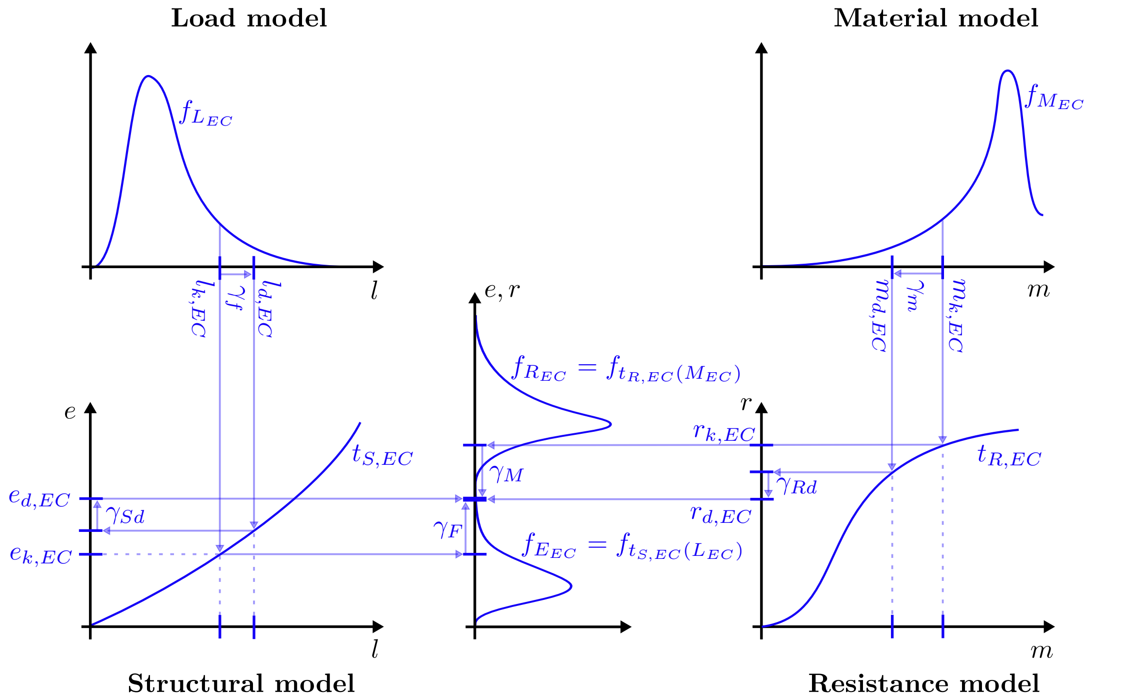

Figure 3: Illustration of the basic reliability problem and its relation to Eurocode models.

of the characteristic values of the Eurocode. A model is conservative in a specific design situation if its prediction leads to a larger design resistance than this reference.

The difference between the Eurocode models and purely aleatoric models is exemplarily illustrated in Figure 4, which re-illustrates Figure 3 including the aleatoric distribution of the load L and the material property M and the functions t_E (true relationship between load and load effect) and t_R (true relationship between material property and resistance). From L and M, the corresponding characteristic values l_k and m_k can be obtained, and, by applying the PSFs, the design values l_d, m_d. Using the functions t_S, t_R, the characteristic values e_k, r_k and the associated design values e_d and r_d are obtained. These are the values to which the respective Eurocode values converge, if all epistemic uncertainties vanish. In this sense, they are the target values of Eurocode models.

In the illustration of Figure 4 each of the Eurocode models is conservative: The load and the material model are conservative because $l_k < l_{k,EC}$ and $m_k > m_{k,EC}$. The structural and the resistance model are conservative because $t_S(l_{d,EC}) < t_{S,EC}(l_{d,EC})$ and

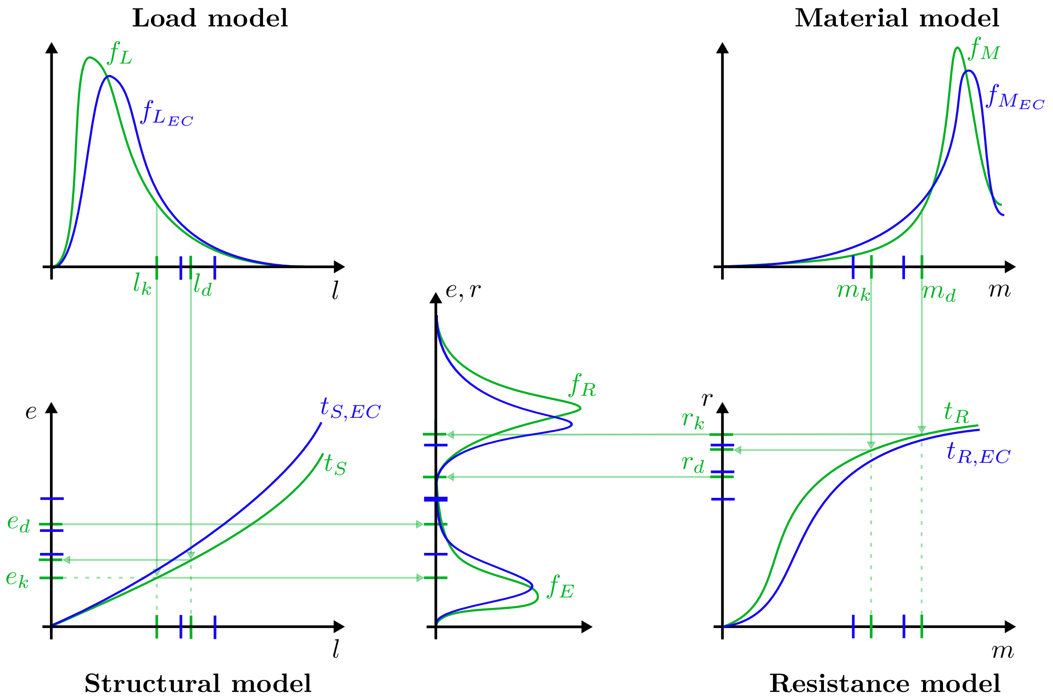

Figure 4: Illustration of the Design approach of the Eurocode (blue) compared to the purely aleatoric models (green) for one specific design situation.

$t_R(m_{d,EC}) > t_{R,EC}(m_{d,EC})$. This leads to an overdesign relative to a design one would obtain from the purely aleatoric models, meaning $r_d < e_d$ while $r_{d,EC} = e_{d,EC}$.

Figure 4 illustrates one specific design situation. If other design situations are considered, the relation between the Eurocode models and the purely aleatoric models may change. Over the domain of all possible design situations, this results in distributions of the characteristic value of the aleatoric distribution of the load L_k and of the material property M_k. Consequently, the characteristic load effect and the characteristic resistance also become random variables E_k and R_k. The transition from L_k and M_k to E_k and R_k is not represented via single functions t_S and t_R beacuse the structural and the resistance model also differ over the domain of all possible design situations. We denote the functionals representing this relationship with T_S and T_R.

For the quantification of the effects of hidden safety, it is crucial to distinguish between:

- The distributions describing the characteristic values of the loads, load effects, material properties, and resistances. These distributions describe variables that enter the design process according to the PSF concept. Hence, they can be used to describe the *design choice* $\mathcal{D}$.

- The distributions describing loads, load effects, material properties, and resistances. These distributions do not enter the design process directly (although the characteristic values result from them). For a given design $\mathcal{D}$, they can be used to perform a *reliability analysis* $\mathcal{R}$ to calculate the aleatoric probability of failure of this design.

For a better understanding of the difference between the distribution of the characteristic value of a phenomenon and the distribution of the phenomenon itself, we illustrate this difference for the wind velocity pressure. The Eurocode defines the characteristic wind velocity pressure $q_{b,k,EC}$ as the value with a yearly exceeding probability of 2 %. Different characteristic values are given by national maps defining wind zones. Within one zone, $q_{b,k,EC}$ is a constant value. Figure 5 plots this constant value against the characteristic value $q_{b,k}$, which follows from the location-specific aleatoric distribution of the wind velocity pressure Q_b. Because the wind velocity pressure fluctuates within one wind zone, this results in a distribution of the characteristic value of the aleatoric distribution $Q_{b,k}$.

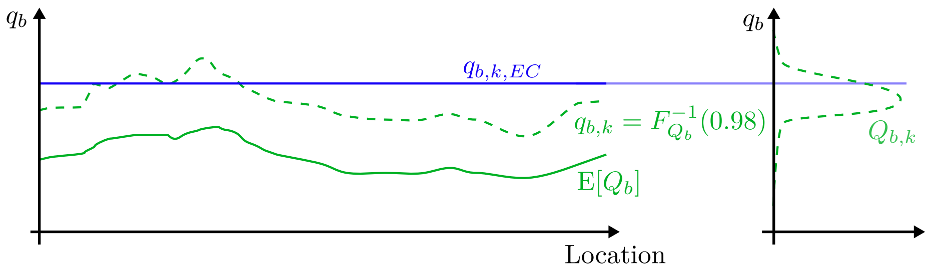

Figure 5: Exemplary illustration of the derivation of the distribution of the characteristic value $Q_{b,k}$ resulting from the aleatoric distribution of the wind velocity pressure Q_b (green) and its relationship to the characteristic value according to Eurocode $q_{b,k,EC}$ (blue).

3.3. Effects of erasing hidden safety

The investigation of hidden safety becomes necessary if more advanced and less conservative models are applied in lieu of standard Eurocode models. To determine how such models affect the reliability, the distributions of the relative errors of the respective models (relative to the characteristic value one would obtain from a purely aleatoric model) are needed.

We illustrate the distribution of the relative errors for the wind velocity pressure. In contrast to Figure 5, we change the perspective by standardizing every quantity relative to $q_{b,k}$. Mathematically, this new perspective is equivalent to the previous one, however, it more clearly reflects how advanced modeling techniques affect the design process. Figure 6 shows this perspective; it also includes the characteristic wind velocity pressure according to advanced modeling techniques $q_{b,k,adv}$, which are shown in red.

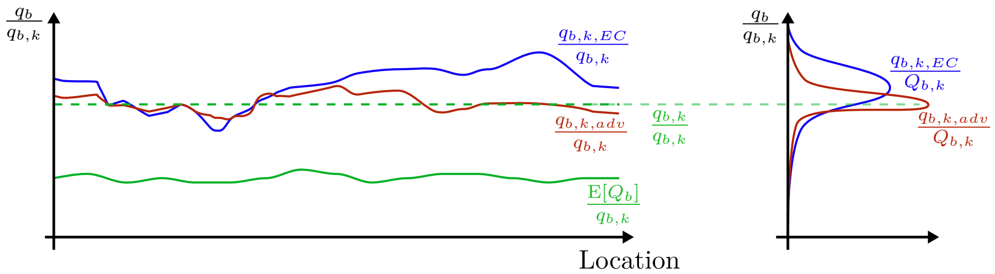

Figure 6: Re-illustration of Figure 5, whereby the wind velocity pressure Q_b (green) and the characteristic value according to Eurocode $q_{b,k,EC}$ (blue) are standardized by the characteristic value of the aleatoric distribution. The characteristic value according to advanced modeling techniques $q_{b,k,adv}$ is added in red.

The distributions of the relative errors (Figure 6 right) can be difficult to estimate. The uncertainty of the involved models needs to be well understood (e.g. as in [41] or [42]). We illustrate the estimation of these distributions for the case of the Eurocode wind load model in Section 4.

By comparing the distributions of $\frac{q_{b,k,EC}}{Q_{b,k}}$ and $\frac{q_{b,k,adv}}{Q_{b,k}}$, the two contradictory effects of advanced modeling techniques on the structural reliability can be identified:

- The decrease of epistemic uncertainty resulting from the use of advanced models reduces the variance of $\frac{q_{b,k,adv}}{Q_{b,k}}$ relative to $\frac{q_{b,k,EC}}{Q_{b,k}}$. This leads to an **increase in the reliability**.

- The decrease of epistemic uncertainties reduces the bias of $\frac{q_{b,k,adv}}{Q_{b,k}}$ relative to $\frac{q_{b,k,EC}}{Q_{b,k}}$. If $\frac{q_{b,k,EC}}{Q_{b,k}}$ is biased in a conservative sense, this leads to a **decrease of the reliability**.

3.4. Quantification of the effects of erasing hidden safety

The effect of replacing the Eurocode model $\mathcal{M}_{EC}$ with an advanced model $\mathcal{M}_{adv}$ is assessed at two levels: First, by comparing the resulting designs; second, by comparing the corresponding aleatoric probability of failure.

The Eurocode model consists of the four components: $\mathcal{M}_{EC} = \{\mathcal{M}_{L,EC}, \mathcal{M}_{S,EC}, \mathcal{M}_{M,EC}, \mathcal{M}_{R,EC}\}$. The advanced model exchanges one or more of these components. For illustration, in this section, we exchange the load model so that $\mathcal{M}_{adv} = \{\mathcal{M}_{L,adv}, \mathcal{M}_{S,EC}, \mathcal{M}_{M,EC}, \mathcal{M}_{R,EC}\}$.

3.4.1. Comparison at design level

In the PSF concept, a design is optimally chosen such that the design resistance is equal to the design load effect. Let $\mathcal{D}_{EC}$ and $\mathcal{D}_{adv}$ be design choices following $\mathcal{M}_{EC}$ and $\mathcal{M}_{adv}$. From Equation 8 and 9, the optimal designs are obtained as:

$$\gamma_{Sd} \cdot T_{S,EC}(L_{k,EC} \cdot \gamma_f) = \frac{T_{R,EC}\left(\frac{M_{k,EC}}{\gamma_m}, \mathcal{D}_{EC}\right)}{\gamma_{Rd}} \tag{10}$$

$$\gamma_{Sd} \cdot T_{S,EC}(L_{k,adv} \cdot \gamma_f) = \frac{T_{R,EC}\left(\frac{M_{k,EC}}{\gamma_m}, \mathcal{D}_{adv}\right)}{\gamma_{Rd}} \tag{11}$$

$L_{k,EC}$, $L_{k,adv}$ and $M_{k,EC}$ are random variables representing the characteristic values standardized to the characteristic values of the respective aleatoric distribution (Figure 6). Their distributions can be derived from those of their respective relative errors.

It is convenient to assume that the design choices $\mathcal{D}_{EC}$ and $\mathcal{D}_{adv}$ can be expressed through factors $\mathcal{P}_{EC}$ and $\mathcal{P}_{adv}$ relative to a standardized design $\mathcal{D}_0$. If the resistance models are linear functions with respect to the design choices $\mathcal{D}_{EC}$ and $\mathcal{D}_{adv}$, Equations 10 and 11 can be reformulated as:

$$\begin{aligned} &\gamma_{Sd} \cdot T_{S,EC}(\gamma_f \cdot L_{k,EC}) = \mathcal{P}_{EC} \cdot \frac{T_{R,EC}\left(\frac{M_{k,EC}}{\gamma_m},\mathcal{D}_0\right)}{\gamma_{Rd}} \\ \Leftrightarrow &\mathcal{P}_{EC} = \frac{\gamma_{Sd} \cdot \gamma_{Rd} \cdot T_{S,EC}(\gamma_f \cdot L_{k,EC})}{T_{R,EC}\left(\frac{M_{k,EC}}{\gamma_m},\mathcal{D}_0\right)} \end{aligned} \tag{12}$$

$$\begin{aligned} &\gamma_{Sd} \cdot T_{S,EC}(\gamma_f \cdot L_{k,adv}) = \mathcal{P}_{adv} \cdot \frac{T_{R,EC}\left(\frac{M_{k,EC}}{\gamma_m},\mathcal{D}_0\right)}{\gamma_{Rd}} \\ \Leftrightarrow &\mathcal{P}_{adv} = \frac{\gamma_{Sd} \cdot \gamma_{Rd} \cdot T_{S,EC}(\gamma_f \cdot L_{k,adv})}{T_{R,EC}\left(\frac{M_{k,EC}}{\gamma_m},\mathcal{D}_0\right)} \end{aligned} \tag{13}$$

$\mathcal{P}_{EC}$ and $\mathcal{P}_{adv}$ are analog to Equation "6.10" of Eurocode 0 [43]; however, models are explicitly included.

The difference of the resistances of the two designs can be measured as the ratio of $\mathcal{P}_{adv}$ over $\mathcal{P}_{EC}$. This ratio is an indication of the reduction in material consumption. It should be noted that the relationship between the design value and the material consumption is not necessarily linear. Moreover, serviceability limit states is not considered.

3.4.2. Comparison at reliability level

For given design values $\mathcal{P}_{adv}$ and $\mathcal{P}_{EC}$, the corresponding aleatoric probability of failure can be computed:

$$\Pr(F \mid \mathcal{P}_{EC},\mathcal{R}) = \Pr(\mathcal{P}_{EC} \cdot T_R(M) - T_S(L) < 0) \tag{14}$$

$$\Pr(F \mid \mathcal{P}_{adv},\mathcal{R}) = \Pr(\mathcal{P}_{adv} \cdot T_R(M) - T_S(L) < 0) \tag{15}$$

Here, the conditioning on $\mathcal{R} = \mathcal{R}(L,T_S,M,T_R)$ indicates that the aleatoric distributions are used.

The values $\Pr(F \mid \mathcal{P}_{EC},\mathcal{R})$ and $\Pr(F \mid \mathcal{P}_{adv},\mathcal{R})$ serve as a comparison of the reliability obtained with the two models.

Remark: Alternatively, the nominal probabilities of failure would be computed with $\mathcal{R}_{EC} = \mathcal{R}(L_{EC}, T_{S,EC}, M_{EC}, T_{R,EC})$ or $\mathcal{R}_{adv} = \mathcal{R}(L_{adv}, T_{S,EC}, M_{EC}, T_{R,EC})$. A comparison of the nominal probabilities of failure with the probabilities of failure calculated via Equation 14 and 15 can be utilized to to quantify the misjudgment of the models being used in the design process. Gomes and Beck [22] propose such a comparison and derive a conservatism index.

3.5. Adaptation of the partial safety factor concept

If advanced models are used in the design process, the PSF concept should be adapted. When replacing load or material models, this adaptation can be conducted by changing either the respective PSFs γ_f, γ_m or the definition of the characteristic values $L_{k,EC}$, $M_{k,EC}$. When replacing structural or resistance models, the PSFs γ_{Sd} and γ_{Rd} can be adapted.

Assuming that the reliability of the status quo is satisfactory, the adaptation should be performed under the constraint of preserving this level of reliability. For example, an additional PSF regarding a load model $\gamma_{f,add}$ can be found by solving the following equation:

$$\Pr(F \mid \mathcal{P}_{EC},\mathcal{R}) = \Pr(F \mid \mathcal{P}_{adv,add}(\gamma_{f,add}),\mathcal{R}) \tag{16}$$

where

$$\mathcal{P}_{adv,add}(\gamma_{f,add}) = \frac{\gamma_{Sd} \cdot \gamma_{Rd} \cdot T_{S,EC}(\gamma_{f,add} \cdot \gamma_f \cdot L_{k,adv})}{T_{R,EC}\left(\frac{M_{k,EC}}{\gamma_m}, \mathcal{D}_0\right)} \tag{17}$$

The aleatoric probabilities of failure of designs resulting from the standard and the advanced modeling techniques are both calculated with the aleatoric distributions (reliability analysis $\mathcal{R}$). Inaccuracies in the assumed aleatoric distributions will affect both probabilities of failure. It is reasonable to presume that both probabilities are affected similar. This makes a relative comparison valid.

The use of PSFs and characteristic values is meaningful mainly when considering a portfolio of design situations. Hence, the adaptation should cover the full spectrum of design situations of which the advanced model is intended to be used. The definition of one possible portfolio can be found in the Annex A.

The proposed adaptation of the partial safety concept is conditional on the estimated distributions of the design values, the assumed aleatoric distributions, and the representation of the portfolio of design situations. Moreover, some uncertainties might be unknown or intentionally omitted (e.g., human errors are typically not considered [44]). The derived reliabilities are dependent on these assumptions. Imperfect assumptions and simplifications might lead to a non-ideal adaptation of the PSF concept. However, the assumptions and simplifications are utilized for both, the calculation of the probability of failure given standard design and given advanced design (Equation 16: The probabilities of failure are both conditional on the same reliability analysis $\mathcal{R}$). This makes the calibration procedure relatively robust. The resulting adaptation may not be ideal; however, it is a step in the right direction and better than performing no adaptation at all.

3.6. Summery of the framework

The following summarizes the proposed framework for treating hidden safety when advanced models are implemented in the PSF concept.

1. Definition of a representative portfolio of design situations the advanced model is intended. This includes the definition of purely aleatoric distributions associated with these design situations.

2. Estimation and determination of the distribution of the relative error by the standard model.

3. Determination of the design following the standard model for all design situations within the considered portfolio.

4. Calculation of the target probability of failure as the avarage aleatoric probability of failure given standard design within the portfolio.

5. Estimation and determination of the distribution of the advanced model.

6. Determination of the design following the advanced model for all design situations within the considered portfolio.

7. Adaptation of the PSF-Concept by adopting PSF or quantile values to define characteristic values, such that the expected aleatoric probability of failure given advanced design is equal to the target probability of failure.

4. Application example: Investigation of hidden safety in the Eurocode wind load model

We exemplify the treatment of hidden safety for the wind load model of Eurocode 1 [45]. We consider an exchange of the Eurocode wind load model $\mathcal{M}_{Wind,EC}$ with more advanced modeling techniques $\mathcal{M}_{Wind,adv}$ and study the effect on the structural reliability and the material usage. In a second step, we adapt the safety components of the Eurocode to achieve the same level of safety with $\mathcal{M}_{Wind,adv}$ than with $\mathcal{M}_{Wind,EC}$. We then re-evaluate the material usage. In order to draw general conclusions, we investigate a portfolio of idealized but representative design situations. The assumptions

4.1. The wind load model of the Eurocode

The wind load model of the Eurocode is based on five components [38, 46]: The wind climate, the terrain, the aerodynamic response, the mechanical response, and the design criteria. Accordingly, Eurocode 1 [45] and its background documentations (e.g., [47]) define the characteristic wind load pressure $q_{k,EC}$ as:

$$q_{k,EC} = q_{b,k,EC} \cdot c_{e,k,EC} \cdot c_{f,k,EC} \cdot c_{s,k,EC} \cdot c_{d,k,EC} \tag{18}$$

These coefficients are characteristic values of the wind load components. Table 1 summarizes the definitions of these characteristic values in Eurocode.

- $q_{b,k,EC}$ is the characteristic value of the wind velocity pressure: It is defined as the 10 minute mean velocity pressure at a height of 10 m above ground with a roughness length of 0.05 m and a return period of 50 years.

- $c_{e,k,EC}$ is the characteristic value of the exposure coefficient: It considers the roughness of the terrain and the height of the structure and is based on empirically determined formulas. Eurocode assumes that these formulas are unbiased estimators of the expected exposure coefficient and thus the characteristic value is the mean.

- $c_{f,k,EC}$ is the characteristic value of the force coefficient: It addresses the geometry of the structure. Its values are based on investigations of [39] and obtained as the 78 % quantile of the yearly maxima of the force coefficient, which are assumed to follow a Gumbel distribution [48].

- $c_{sd,k,EC} := c_{s,k,EC} \cdot c_{d,k,EC}$ is the characteristic value of the structural factor: It accounts for the fact that wind peak pressures do not occur simultaneously on the total surface of the structure (represented through c_s) and for the dynamical effect caused by wind turbulences exciting the structure at its eigenfrequencies (represented through c_d). Eurocode assumes that these formulas are unbiased estimators of the expected structural factor and thus the characteristic value is the mean.

$q_{b,k,EC} = F^{-1}_{Q_{b,EC}}(0.98)$
$c_{e,k,EC} = \mathrm{E}[C_{e,EC}]$
$c_{f,k,EC} = F^{-1}_{C_{f,EC}}(0.78)$
$c_{sd,k,EC} = \mathrm{E}[C_{sd,EC}]$

Table 1: Characteristic values of the wind load model components according to Eurocode.

The four wind load model components ($q_{b,k,EC}$, $c_{e,k,EC}$, $c_{f,k,EC}$ and $c_{sd,k,EC}$) are estimates of quantile values of the respective underlying aleatoric distributions. Here, only the standardized aleatoric distribution will be needed; hence we set their means to 1. Following [49] and [16], we define the coefficients of variations (c.o.v.) of the aleatoric distributions in Table 2.

	Mean	c. o. v.
$Q_b \sim \mathcal{G}$	1	0.25
$C_e \sim \mathcal{LN}$	1	0.15
$C_f \sim \mathcal{G}$	1	0.10
$C_{sd} \sim \mathcal{LN}$	1	0.10

Table 2: Standardized aleatoric distributions of wind load model components. The maximum wind velocity pressure Q_b refers to an annual reference period.

The aleatoric distributions are used when computing the reliability of a design according to the Eurocode wind load model and according to the advanced wind load modeling techniques. The accuracy of the aleatoric distributions is therefore not crucial because a relative comparison is still reasonable.

4.2. Distributions of the characteristic wind load model components according to the Eurocode

Table 3 summarizes the distributions of the inverse relative errors of the Eurocode models. The justification of the distribution choices can be found in Annex B. The characteristic value of aleatoric distribution is known from the assumed aleatoric distributions; hence, by rearranging $\Theta^{-1} = \frac{\text{Characteristic value of aleatoric distribution}}{\text{Characteristic value of EC}}$ the probability distributions of the characteristic values of Eurocode wind load model components can be derived.

	Mean	c. o. v.
$\Theta^{-1}_{q_{b,k,EC}} \sim \mathcal{LN}$	0.8	0.30
$\Theta^{-1}_{c_{e,k,EC}} \sim \mathcal{LN}$	0.8	0.15
$\Theta^{-1}_{c_{f,k,EC}} \sim \mathcal{LN}$	0.9	0.20
$\Theta^{-1}_{c_{sd,k,EC}} \sim \mathcal{LN}$	1.0	0.15

Table 3: Distribution of the relative errors $\frac{\text{Characteristic value of aleatoric distribution}}{\text{Characteristic value of EC}}$.

4.3. Distributions of the characteristic wind load model components according to advanced modeling techniques

We assume that advanced wind load modeling techniques use on-site wind data and perform wind tunnel tests. The structure of the wind load model still follows the Eurocode approach, meaning that the wind is still modeled by means of a wind velocity pressure $q_{b,k,adv}$, an exposure coefficient $c_{e,k,adv}$, a force coefficient $c_{f,k,adv}$, and a structural factor $c_{sd,k,adv}$. Table 4 summarizes the distributions of the inverse relative errors of the advanced models. The justification of the distribution choices can be found in Annex C. The derived distributions depend on certain assumptions on the advanced wind load modeling; however, there is a great variety and a constant development in advanced wind load modeling techniques (e.g. [50]). Therefore, each individual case should revise the derived distributions.

The respective distributions of the characteristic values of wind load model components according to advanced wind load modeling techniques are derived by rearranging $\Theta^{-1} = \frac{\text{Characteristic value of aleatoric distribution}}{\text{Characteristic value of Adv}}$.

	Mean	c. o. v.
$\Theta^{-1}_{q_{b,k,adv}} \sim \mathcal{LN}$	1.0	0.10
$\Theta^{-1}_{c_{e,k,adv}} \sim \mathcal{LN}$	1.0	0.05
$\Theta^{-1}_{c_{f,k,adv}} \sim \mathcal{LN}$	1.0	0.15
$\Theta^{-1}_{c_{sd,k,adv}} \sim \mathcal{LN}$	1.0	0.10

Table 4: Distribution of the relative errors $\frac{\text{Characteristic value of aleatoric distribution}}{\text{Characteristic value of Adv}}$.

4.4. Numerical investigations

We apply $\mathcal{M}_{Wind,EC}$ and $\mathcal{M}_{Wind,adv}$ to the portfolio of representative design situations described in Annex A. In the case of advanced wind load modeling, we distinguish five cases: Four cases in which only one of the advanced wind load models is applied and one combined case in which all four advanced wind load models are applied simultaneously. We investigate the effects of erasing hidden safety on the design and on the reliability. In a second step, we adapt the PSF concept as described in Section 3.5 and re-evaluate the resulting design.

4.4.1. Effect on the design

We investigate the effect on the design via a relative comparison of design values (Equation 12 and 13). Violin plots of the resulting distributions are shown in Figure 7. Ratios of the expected value of the design according to the advanced model cases to the Eurocode model case are reported in Table 5.

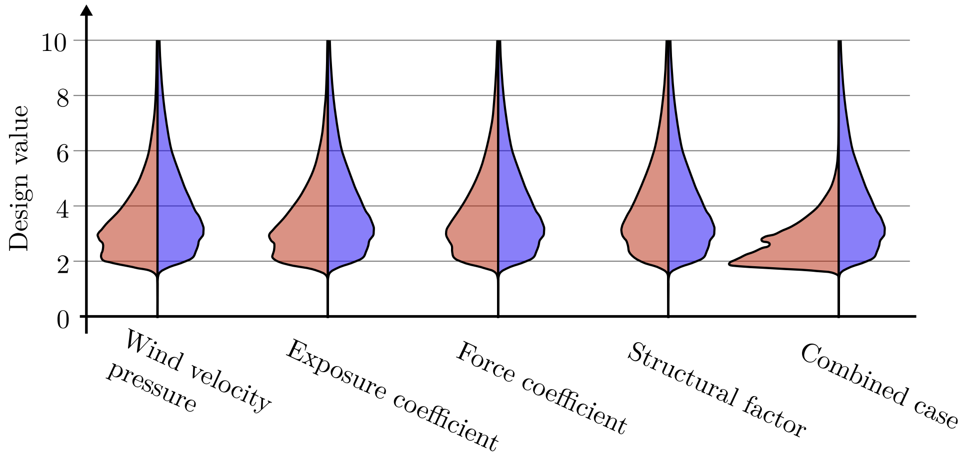

Figure 7: Violin plots showing the distribution of design values obtained with Eurocode models (blue) and advanced models (red).

Wind velocity pressure	0.80
Exposure coefficient	0.84
Force coefficient	0.92
Structural factor	1.00
Combined case	0.62

Table 5: Average design values obtained with the use of advanced modeling techniques relative to those obtained with Eurocode models.

4.4.2. Effect on reliability

Given the distributions of the design values, we investigate how the aleatoric probability of failure changes when moving from Eurocode models to advanced models. The aleatoric probability of failure is calculated with the first-order reliability method (FORM) [51]. Figure 8 shows box plots of the resulting reliability indices. Ratios of the expected values of the aleatoric probabilities of failure of the advanced model cases to the ones of the Eurocode model case are reported in Table 6.

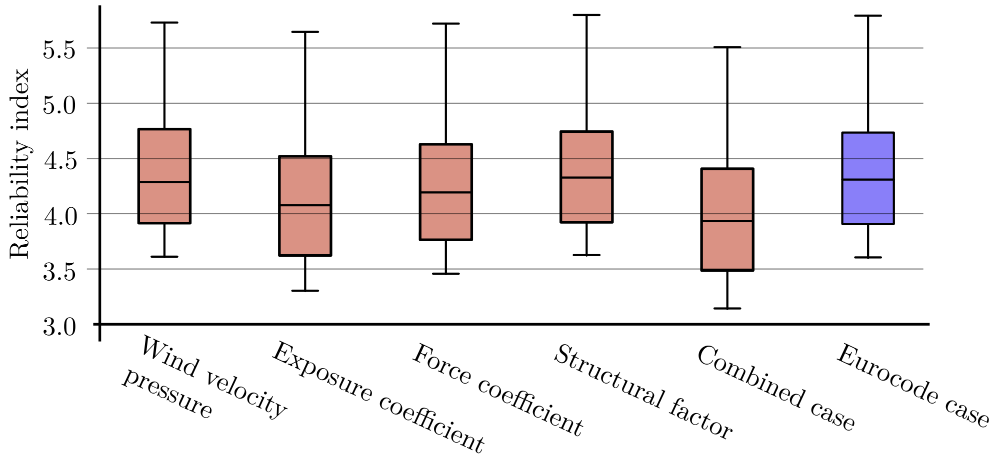

Figure 8: Boxplots of the annual reliability indices according to Eurocode (blue) and advanced modeling techniques (red).

Wind velocity pressure	1.08
Exposure coefficient	3.05
Force coefficient	1.50
Structural factor	0.80
Combined case	4.22

Table 6: Ratios of the weighted averaged annual probabilities of failure of the design following Eurocode and advanced modeling techniques.

4.4.3. Adaptation of the partial safety factor concept

To compensate the lost hidden safety through the application of advanced modeling techniques, we adapted either the PSF of the wind load or the characteristic values of each wind load model component. We demonstrate both; however, the latter only for the characteristic wind velocity pressure.

The adaptation is conducted under the constraint of equal aleatoric probability of failures. An annual target probability of failure is calculated as the expected aleatoric probability of failure with respect to the different design situations of the portfolio.

$$p_{F_{TRG}} = \mathrm{E}\left[\Pr(F \mid \text{EC-Design})\right] = 3 \cdot 10^{-5} \tag{19}$$

- Adaptation of the PSF:

  We adapt $\gamma_Q = 1.5$ of wind by introducing an additional PSF of $\gamma_{Q,add}$ which is found by solving the following equation:

$$\mathrm{E}\left[\Pr(F \mid \text{Adv-Design including } \gamma_{Q,add}\ )\right] = \Pr(F)_{TRG} \tag{20}$$

  The additional PSFs are also calculated for the cases where only one of the wind load model components is derived from advanced techniques. Table 7 shows the resulting additional PSFs. Values above 1 result in an increase of γ_Q, values bellow 1 decrease γ_Q.

Wind velocity pressure:	1.01
Exposure coefficient:	1.19
Force coefficient:	1.06
Structural factor:	0.97
Combined case:	1.20

Table 7: Additional PSF $\gamma_{Q,add}$ regarding each advanced wind load modeling technique and the combined case.

- The adaptation of the quantile value defining the characteristic wind velocity pressure was conducted such that

$$\mathrm{E}\left[\Pr(F \mid \text{Adv-Design with new quantile value})\right] = \Pr(F)_{TRG} \tag{21}$$

  This resulted in a quantile of 0.9817 instead of 0.98.

Remark: We also conducted the adaptation under the constraint of equal reliability indices.

The target reliability index is calculated as the expected reliability index with respect to the different design situations of the portfolio. This is significantly higher than the reliability index, which corresponds to the target probability of failure (4.39 instead of $4.01 = -\Phi^{-1}(p_{F_{TRG}})$). However, the adaptation is also be conducted in the transformed domain of reliability indices. The resulting difference in the additional PSFs and the adopted quantile value defining the characteristic wind velocity pressure is negligible.

4.4.4. Effects of the adaptation

The adaptation of the safety factors is introduced in order to ensure that the overall reliability achieved with the advanced model is the same as the one of the Eurocode model. Here, we investigate the effect of this adaptation on the material usage achieved with advanced models.

Table 8 shows the ratio of weighted averaged expected values of design values with an adapted PSF. Comparing these values to the ratios without adaptation (last row in Table 5), it can be seen that the adaptation leads to a (albeit limited) reduction of the material savings from the use of advanced wind load modeling techniques.

Wind velocity pressure	0.81
Exposure coefficient	0.95
Force coefficient	0.95
Structural factor	0.97
Combined case	0.70

Table 8: Average design values obtained with the use of advanced modeling techniques relative to those obtained with Eurocode models with adapted PSFs.

If the quantile value that defines the characteristic wind velocity pressure is adapted, the material saving potential is marginally better then in the case of an additional PSF with respect to an advanced model regarding the wind velocity pressure: The ratio of the averaged design values decreases from 0.81 to 0.80.

5. Concluding remarks

Structural design codes are the result of a long evolutionary adaptation process. This adaptation is partly empirical (through the inclusion of new experience) and partly deductive (through the use of new and advanced models). The empirical adaptation of design codes mostly retains the hidden safety arising from conservative choices in model parameters. In contrast, a deductive adaptation typically changes the amount of hidden safety. In this paper, we propose a framework to compensate for such changes in hidden safety in order to ensure a consistent overall safety level.

The framework can be used to account for hidden safety within the partial safety concept when advanced modeling techniques replace standard models. This will typically result in – on average – lower design values while still achieving the same level of safety. It may seem counter-intuitive that the average reliability remains unchanged if the resistances are reduced on average; however, this is due to the more targeted designs (i.e., the design is strengthened where it is needed, and relaxed where it is not).

The application of the proposed framework is based on model assumptions as it is the case for any code calibration. These assumptions might not be fully correct; hence, the resulting calibration may not be optimal. However, it is still a step in the right direction and preferable to the applications of advanced models without a calibration through the proposed framework.

The most challenging part of in investigations of hidden safety is the evaluation of the accuracy of the standard and the advanced model. The probabilistic description of these accuracies is challenging because they characterize the model prediction relative to the "truth". However, the truth is unknown. Empirical data and expert knowledge must be taken into account carefully. The quantification of the effect of hidden safety and the calibration of the PSF concept are sensitive to the probability distributions describing model accuracies.

The choice of a representative portfolio of design situations and an adequate probabilistic description of all random variables within the portfolio may seem to be another critical point. However, the calibration of safety components is not sensitive to the portfolio choices. This is because the portfolio is used for the investigation of both the standard model and the advanced model. This validates a relative comparison – which is the basis of the calibration – of the two models valid, even if the portfolio is not perfectly accurate.

The study of Section 4 to investigation the effects of hidden safety in the wind load model of Eurocode are an exemplary application of the framework introduced in the previous sections. Importantly, the additional safety factor to be used depends on the actual model used in a specific application.

The exemplary study results in a decrease of the average design value to 70 %. This is equivalent to a design load reduction of 30 %. The reduction of the average design wind load is even higher because the load within the portfolio is a mixture of wind load, self weight and permanent loads. However, when calculating the average design value the self weight and the permanent loads do not differ with respect to the Eurocode model or the advanced wind load modeling techniques.

The decrease of the average design value to 70 % is not equivalent to a reduction of the material effort of 30 % for the following two reasons: First, the relationship between the design value and the material effort depends on the design situation (e.g., for trusses under pure tension, the relationship is a one-to-one mapping, but the bending resistance of a rectangular beam has quadratic relationship with the material effort). Second, the design values are calculated only with respect to the ultimate limit states involving wind load cases. Other ultimate and serviceability limit states are not included. This suggests that the reduction in material usage would be less than 30 %.

In general, investigations of the effects of hidden safety are necessary if advanced models – which are not covered by the codes – are used. With the rapid developments of computational engineering, such use is increasingly frequent. Engineers who use these newly developed models may have the impression that their designs have increased reliability because the advanced models are more precise. However, because of hidden safeties this does not necessarily have to be the case. The proposed framework ensures that semi-probabilistic design codes are calibrated such that the advanced models and the established models lead to the same level of safety. The higher accuracy of advanced models is still utilized and translated into a higher material efficiency. This results in more sustainable and economic structures that are equally safe. Because the building industry is one of the main material and energy consumers and is responsible for a high amount of greenhouse gas emissions, it is essential to utilize this material saving potential.

References

[1] Ove Ditlevsen and Henrik Madsen. *Structural Reliability Methods.* Wiley New York, 1996.

[2] Victor Saouma. *Lecture Notes: Structural Engineering–Analysis and Design.* University of Colorado: Dept. of Civil Environmental and Architectural Engineering, 2016.

[3] Jacques Heyman and Heyman Jacques. *Structural Analysis: A Historical Approach.* Cambridge University Press, 1998.

[4] Hans Straub. *Die Geschichte der Bauingenieurkunst [The history of civil engineering].* Springer-Verlag, 2013.

[5] Karl-Eugen Kurrer. *Geschichte der Baustatik [History of structural analysis].* John Wiley & Sons, 2002.

[6] Peter Marti. *Baustatik: Grundlagen, Stabtragwerke, Flächentragwerk [Structural analysis: Fundamentals, beam structures, shell structures].* John Wiley & Sons, 2012.

[7] Bruce Ellingwood, Theodore Galambos, and James MacGregor. *Development of a Probability Based Load Criterion for American National Standard A58: Building Code Requirements for Minimum Design Loads in Buildings and Other Structures.* Department of Commerce, National Bureau of Standards, 1980.

[8] Theodore Galambos, Bruce Ellingwood, James MacGregor, and Allin Cornell. Probability Based Load Criteria: Assessment of Current Design Practice. *Journal of the Structural Division*, 108(5):959–977, 1982.

[9] Bruce Ellingwood, James MacGregor, Theodore Galambos, and Allin Cornell. Probability Based Load Criteria: Load Factors and Load Combinations. *Journal of the Structural Division*, 108(5):978–997, 1982.

[10] Rüdiger Rackwitz. *Vorlesungsskript: Zuverlässigkeit und Lasten im konstruktiven Ingenieurbau [Lecture notes: Reliability and Loads in Structural Engineering].* Technische Universität, München, 2004.

[11] Deutsches Institut für Normung. *GruSiBau: Grundlagen zur Festlegung von Sicherheitsanforderungen für bauliche Anlagen [GruSiBau: Basic principles for the definition of safety requirements for structures].* Beuth Verlag, 1981.

[12] Robert Melchers and André Beck. *Structural Reliability Analysis and Prediction.* John Wiley & Sons, 2018.

[13] Henrik Madsen, Steen Krenk, and Niels Christian Lind. *Methods of Structural Safety.* Courier Corporation, 2006.

[14] Michael Faber and John Sørensen. Reliability-Based Code Calibration: The JCSS Approach. *Proceedings of the 9th International Conference on Applications of Statistics and Probability in Civil Engineering*, 9:927–935, 2003.

[15] Michele Baravalle. *Risk and Reliability Based Calibration of Structural Design Codes.* PhD thesis, Norwegian University of Science and Technology, 2017.

[16] Jochen Köhler, Michele Baravalle, and John Sørensen. Calibration of existing semi-probabilistic design codes. *Proceedings of the 13th International Conference on Applications of Statistics and Probability in Civil Engineering*, 2019. `doi:10.22725/ICASP13.325`.

[17] John Anderson and John Wendt. *Computational Fluid Dynamics.* Springer, 1995.

[18] Yousef Bozorgnia and Vitelmo Bertero. *Earthquake Engineering: From Engineering Seismology to Performance-Based Engineering.* CRC press, 2004.

[19] Mike Byfield and David Nethercot. Eurocodes - failing to standardise safety. *Proceedings of the Institution of Civil Engineers-Civil Engineering*, 144(4):186–188, 2001. `doi:10.1680/cien.2001.144.4.186`.

[20] Milan Holicky, Johan Retief, and Celeste Viljoen. Partial Factors for Wind Actions Considering Hidden Safety due to Time Invariant Components. *Proceedings of the 6th International Conference on Structural Engineering, Mechanics and Computation*, 6:687–692, 2016.

[21] Andrzej Nowak and Bala Tharmabala. Bridge Reliability Evaluation Using Load Tests. *Journal of Structural Engineering*, 114(10):2268–2279, 1988.

[22] Wellison José de Santana Gomes and André Beck. A conservatism index based

on structural reliability and model errors. *Reliability Engineering & System Safety*, 209:107456, 2021. doi:10.1016/j.ress.2021.107456.

[23] Henrik Toft, Kim Branner, John Sørensen, and Peter Berring. Reliability-based Calibration of Partial Safety Factors for Wind Turbine Blades. *The European Wind Energy Association: Europe's Premier Wind Energy Event: scientific proceedings*, (5):124–128, 2011.

[24] Maria Hänninen, Osiris Banda, and Pentti Kujala. Bayesian network model of maritime safety management. *Expert Systems with Applications*, 41(17):7837–7846, 2014. doi:10.1016/j.eswa.2014.06.029.

[25] George Gazetas, Ioannis Anastasopoulos, and Evangelia Garini. Geotechnical design with apparent seismic safety factors well-bellow 1. *Soil Dynamics and Earthquake Engineering*, 57:37–45, 2014. doi:10.1016/j.soildyn.2013.10.002.

[26] Johnny Henderson and David Blockley. Logical analysis of assumptions in code calibration. *Structural Safety*, 1(2):123–140, 1982. doi:10.1016/0167-4730(82)90020-0.

[27] John Sørensen. Calibration of partial safety factors in danish structural codes. *JCSS Workshop on Reliability Based Code Calibration*, 21(22.03):2002, 2002.

[28] Armen Der Kiureghian and Ove Ditlevsen. Aleatory or epistemic? does it matter? *Structural safety*, 31(2):105–112, 2009. doi:10.1016/j.strusafe.2008.06.020.

[29] Nancy Cartwright and Ernan McMullin. *How the laws of physics lie*. American Association of Physics Teachers, 1984.

[30] Nancy Cartwright. Fundamentalism vs. the patchwork of laws. *Proceedings of the*

Aristotelian Society, 94:279–292, 1994.

[31] Nancy Cartwright. Nature's capacities and their measurement. *OUP Catalogue*, 1994. `doi:10.1093/0198235070.001.0001`.

[32] Daniela M Bailer-Jones. *Scientific models in philosophy of science.* University of Pittsburgh Pre, 2009.

[33] Ludwig Wittgenstein. *Tractatus logico-philosophicus.* Routledge, 2013.

[34] Martin Heidegger. *Sein und Zeit [Being and time].* Halle ad S.: M. Niemeyer, 1927.

[35] Karl Jaspers. *Psychologie der Weltanschauungen [Psychology of worldviews].* Springer-Verlag, 2013.

[36] Immanuel Kant. *Kritik der reinen Vernunft [Critique of Pure Reason].* Mayer & Müller, 1889.

[37] Diego Lorenzo Allaix, Vincenzo Ilario Carbone, and Giuseppe Mancini. Global safety format for non-linear analysis of reinforced concrete structures. *Structural concrete*, 14(1):29–42, 2013. `doi:10.1002/suco.201200017`.

[38] Alan Davenport. The relationship of reliability to wind loading. *Journal of Wind Engineering and Industrial Aerodynamics*, 13:3–27, 1983.

[39] Nicholas John Cook. *The Designer's Guide to Wind Loading of Building Structures: Part 1: Background, Damage Survey, Wind Data and Structural Classification.* Butterworth Publishers, 1985.

[40] Wolfgang Grasse. Lasten und Einwirkungen auf Brücken einschließlich Kombination-

sregeln [Loads and actions on bridges including combination rules] (DIN-Fachbericht 101). *Technical University Dresden*, 2009.

[41] Paolo Castaldo, Diego Gino, Gabriele Bertagnoli, and Giuseppe Mancini. Partial safety factor for resistance model uncertainties in 2D non-linear finite element analysis of reinforced concrete structures. *Engineering Structures*, 176:746–762, 2018. `doi:10.1016/j.engstruct.2018.09.041`.

[42] Morten Engen, Max Hendriks, Jochen Köhler, Jan Arve Øverli, and Erik Åldstedt. A quantification of the modelling uncertainty of non-linear finite element analyses of large concrete structures. *Structural safety*, 64:1–8, 2017. `doi:10.1016/j.strusafe.2016.08.003`.

[43] CEN. Eurocode 0: Basis of structural design, 2002.

[44] William M Bulleit. Uncertainty in structural engineering. *Practice Periodical on Structural Design and Construction*, 13(1):24–30, 2008. `doi:10.1061/(ASCE)1084-0680(2008)13:1(24)`.

[45] CEN. Eurocode 1: Actions on structures –part 1-4: general actions, wind actions, 2005.

[46] Alan Davenport. The application of statistical concepts to the wind loading of structures. *Proceedings of the Institution of Civil Engineers*, 19(4):449–472, 1961.

[47] Hans-Juergen Niemann. The European Wind Loading Code: Background and Regulations. *Structures Congress*, :1–9, 2004. `doi:10.1061/40700(2004)61`.

[48] Michele Baravalle and Jochen Köhler. On the probabilistic representation of the wind

climate for calibration of structural design standards. *Structural safety*, 70:115–127, 2018.

[49] Joint Committee on Structural Safety. *The JCSS probabilistic model code*. 2001. URL: https://www.jcss-lc.org/jcss-probabilistic-model-code/.

[50] DongHun Yeo and Arindam Gan Chowdhury. A Simplified Wind Flow Model for the Estimation of Aerodynamic Effects on Small Structures. *Journal of Engineering Mechanics*, 139(3):367–375, 2013. doi:10.1061/(ASCE)EM.1943-7889.0000508.

[51] Rüdiger Rackwitz and Bernd Flessler. Structural reliability under combined random load sequences. *Computers & Structures*, 9(5):489–494, 1978.

[52] CEN. Eurocode 2: Design of concrete structures, 2004.

[53] CEN. Eurocode 3: Design of steel structures, 2005.

[54] CEN. Eurocode 5: Design of timber structures, 2008.

[55] CEN. Eurocode 6: Design of masonry structures, 2006.

[56] Alan Davenport. Proposed new international (ISO) wind load standard. *Second Asia-Pacific Symposium on wind-engineering*, 1:1199–1214, 1989.

[57] Deutscher Wetterdienst (DWD) [German Weather Service]. Wind velocity data. ftp://ftp-cdc.dwd.de/pub/CDC/observations_germany, 2018.

[58] Stuart Coles, Joanna Bawa, Lesley Trenner, and Pat Dorazio. *An Introduction to Statistical Modeling of Extreme Values*. Springer, 2001.

[59] Svend Hansen, Marie Louise Pedersen, and John Sørensen. Probability-based calibration of pressure coefficients. *Proceedings of the 14th International Conference on Wind Engineering*, 2015. doi:10.5359/jawe.40.428.

[60] Robert Wardlaw and G Moss. A standard tall building model for the comparison of simulated natural winds in wind tunnels. *Commonwealth Advisory Aeronautical Council*, 25, 1970.

[61] Working Group on the Expression of Uncertainty in Measurement. *Guide to the Expression of Uncertainty in Measurement*. Joint Committee for Guides in Metrology, 2008.

[62] Niels Sørensen, Andreas Bechmann, Pierre-Elouan Réthoré, Dalibor Cavar, Mark Kelly, and I Troen. How fine is fine enough when doing CFD terrain simulations. *European Wind Energy Association*, 10, 2012.

[63] Mark Kelly and Hans Jørgensen. Statistical characterization of roughness uncertainty and impact on wind resource estimation. *Wind Energy Science*, 2(1):189–209, 2017.

[64] Yen Dora and Braeuchle Frank. Calibration and Uncertainty Analysis for the UC Davis Wind Tunnel Facility. *UC Davis Wind Tunnel Calibration Document*, 2000.

[65] Fei Long. *Uncertainties in pressure coefficients derived from full and model scale data*. PhD thesis, Texas Tech University, 2004.

[66] Marc Levitan and Kishor Mehta. Texas tech field experiments for wind loads part 1 and 2. *Journal of Wind Engineering and Industrial Aerodynamics*, 43(1-3):1565–1576, 1992.

[67] Jill Campbell. *Wind engineering research field laboratory site characterization*. PhD

thesis, Texas Tech University, 1995.

[68] William Fritz, Bogusz Bienkiewicz, Bo Cui, Olivier Flamand, Eric Ho, Hitomitsu Kikitsu, Chris Letchford, and Emil Simiu. International Comparison of Wind Tunnel Estimates of Wind Effects on Low-Rise Buildings: Test-Related Uncertainties. *Journal of structural engineering*, 134(12):1887–1890, 2008. `doi:10.1061/ASCE0733-94452008134:121887`.

A. Definition of a portfolio of representative design situations

In order to draw general conclusions, we apply the distributions of the characteristic values of $\mathcal{M}_{Wind,EC}$ and $\mathcal{M}_{Wind,adv}$ to a portfolio of design situations. The portfolio is specified via a generic limit state function g (following [16]):

$$\begin{aligned} g(p,\Theta_{R_i},R_i,G_{S,i},G_P,Q,a_{Q,i},a_G) =& P_{EC,i} \cdot \Theta_{R_i} \cdot R_i - \\ & - (1 - a_{Q,i}) \cdot [a_G \cdot G_{S,i} + (1 - a_G) \cdot G_P] - a_{Q,i} \cdot Q \end{aligned} \tag{22}$$

This limit state function is valid for a material i. Θ_{R_i} is the resistance model uncertainty, R_i is the material strength, $G_{S,i}$ is the self-weight, G_P is the permanent load and Q represents the wind load. They are normalized values. In order to account for different design situations, the weights $a_{Q,i}$ and a_G allow representing different load compositions. Finally $P_{EC,i}$ is defined as:

$$P_{EC,i} = \frac{\gamma_{R_i}}{\theta_{R_i,k} \cdot r_{i,k}} \cdot [(1 - a_{Q,i}) \cdot (a_G \cdot \gamma_S \cdot g_{S_i,k} + (1 - a_G) \cdot \gamma_P \cdot g_{P,k}) + a_{Q,i} \cdot \gamma_Q \cdot q_k] \tag{23}$$

The definition of $P_{EC,i}$ is in agreement with Equations 12 and 13, whereby the load model is a linear combination of wind load, self-weight, and permanent load. $T_{\mathcal{M}_R}$ is expressed multiplicatively via $\theta_{R_i,k}$, and $T_{\mathcal{M}_S}$ is neglected. Moreover, the PSFs are merged on both, the load and the resistance side.

Six different material properties R_i are considered and weighted with $w_{R,i}$ according to their relative frequency. For each material ranges different load compositions are investigated via $a_{Q,i}$ and a_G(Table 9). Ten equally spaced and equally weighted values of $a_{Q,i}$ are considered and three equally spaced and equally weighted values of a_G are considered. The distributions of each material property R_i, the associated resistance uncertainty Θ_{R_i}, the self weight G_{S_i}, and the permanent load G_P are given in Table 10.

The values of the PSFs follow Eurocode 0 [43] (Table 11). The characteristic values of the wind load following Eurocode and advanced wind load modeling techniques are calculated as:

$$q_{k,EC} = F^{-1}_{Q_{b,EC}}(0.98) \cdot \mathrm{E}[C_{e,EC}] \cdot F^{-1}_{C_{f,EC}}(0.78) \cdot \mathrm{E}[C_{sd,EC}] \tag{24}$$

$$q_{k,adv} = F^{-1}_{Q_{b,adv}}(0.98) \cdot \mathrm{E}[C_{e,adv}] \cdot F^{-1}_{C_{f,adv}}(0.78) \cdot \mathrm{E}[C_{sd,adv}] \tag{25}$$

The remaining characteristic values are chosen following Eurocode 1, 2, 3, 5, 6 [43, 52–55] and the ongoing revision of the Eurocode [16] (Table 12).

i	Material	$w_{R,i}\%$	$a_{Q,i}$ ranges	a_G ranges
1	Steel yielding strength	40.0	$[0.2; 0.8]$	
2	Concrete compression strength	15.0	$[0.1; 0.7]$	
3	Re-bar yielding strength	25.0	$[0.1; 0.7]$	$[0.6; 1.0]$
4	Glulam timber bending strength	7,5	$[0.2; 0.8]$	
5	Solid timber bending strength	2,5	$[0.2; 0.8]$	
6	Masonry compression strength	10.0	$[0.1; 0.7]$	

Table 9: Material properties, weights and ranges of $a_{Q,i}$ and a_G based on [16].

	Mean	c. o. v.
$\Theta_{R_1} \sim \mathcal{LN}$	1.00	0.050
$\Theta_{R_2} \sim \mathcal{LN}$	1.00	0.100
$\Theta_{R_3} \sim \mathcal{LN}$	1.00	0.100
$\Theta_{R_4} \sim \mathcal{LN}$	1.00	0.100
$\Theta_{R_5} \sim \mathcal{LN}$	1.00	0.100
$\Theta_{R_6} \sim \mathcal{LN}$	1.16	0.175
$R_1 \sim \mathcal{LN}$	1.00	0.070
$R_2 \sim \mathcal{LN}$	1.00	0.150
$R_3 \sim \mathcal{LN}$	1.00	0.070
$R_4 \sim \mathcal{LN}$	1.00	0.150
$R_5 \sim \mathcal{LN}$	1.00	0.200
$R_6 \sim \mathcal{LN}$	1.00	0.160
$G_{S_1} \sim \mathcal{N}$	1.00	0.040
$G_{S_2} \sim \mathcal{N}$	1.00	0.050
$G_{S_3} \sim \mathcal{N}$	1.00	0.050
$G_{S_4} \sim \mathcal{N}$	1.00	0.100
$G_{S_5} \sim \mathcal{N}$	1.00	0.100
$G_{S_6} \sim \mathcal{N}$	1.00	0.065
$G_P \sim \mathcal{N}$	1.00	0.100
$Q \sim$ as in Table 2		

Table 10: Aleatoric distributions based on [49] and [16].

i	$\gamma_{R,i}$	γ_S	γ_P	γ_Q
1	1.00			
2	1.50			
3	1.15	1.35	1.35	1.5
4	1.25			
5	1.30			
6	1.50			

Table 11: PSFs according to Eurocode [43].

i	$r_{i,k}$	$g_{S_i,k}$	$\theta_{R_i,k}$	$g_{P,k}$
1	$\mathrm{E}[R_i] - 2 \cdot \sqrt{\mathrm{Var}[R_i]}$	$F_{R_i}^{-1}(0.5)$	$\mathrm{E}[\Theta_{R_i}]$	
2	$F_{R_i}^{-1}(0.05)$	$F_{R_i}^{-1}(0.5)$	$\mathrm{E}[\Theta_{R_i}]$	
3	$F_{R_i}^{-1}(0.05)$	$F_{R_i}^{-1}(0.5)$	$\mathrm{E}[\Theta_{R_i}]$	$F_{G_P}^{-1}(0.5)$
4	$F_{R_i}^{-1}(0.05)$	$F_{R_i}^{-1}(0.5)$	$\mathrm{E}[\Theta_{R_i}]$	
5	$F_{R_i}^{-1}(0.05)$	$F_{R_i}^{-1}(0.5)$	$\mathrm{E}[\Theta_{R_i}]$	
6	$F_{R_i}^{-1}(0.05)$	$F_{R_i}^{-1}(0.5)$	$\mathrm{E}[\Theta_{R_i}]$	

Table 12: Characteristic values according to Eurocode [16, 43, 52–55].

B. Relative errors in the estimation of characteristic wind load model components according to standard models

The distribution parameters of table 3 are justified as follows:

- $\Theta^{-1}_{q_{b,k,EC}}$: Davenport [56] suggests a mean value of 0.8 and a coefficient of variation of 0.2–0.3. In order to verify these numbers, we investigate the wind velocity v_b at 10 m above ground of 265 meteorological stations of the German Meteorological Service [57]. Each of the stations is located in open space. Only stations between 0–1100 m above sea level (range of validity of the Eurocode) and only stations with at least 20 years of recording are considered. The wind velocity is converted to the wind velocity pressure via

$$q_b = \frac{1}{2} \cdot \rho \cdot v_b^2 \tag{26}$$

  where $\rho = 1.25\,\frac{\mathrm{kg}}{\mathrm{m}^3}$ is the air density. From the time histories of q_b, the yearly maxima at all stations are obtained and used to fit a Gumbel distribution through a maximum likelihood estimator. We account for the statistical uncertainty via a normal approximation of the posterior [58]. Finally, we obtain $q_{b,k,Data}$ as the 98 % quantiles of each Gumbel distribution and divide them by the characteristic values of the respective location specified in the Eurocode. The resulting ratios are shown in Figure 9. The sample mean of these ratios is 0.82, which confirms the choice of $\mathrm{E}[\Theta^{-1}_{q_{b,k,EC}}] = 0.8$. The sample coefficient of variation is 0.36. We therefore choose the upper bound of the values suggested by Davenport [56].

- $\Theta^{-1}_{c_{e,k,EC}}$: Davenport [56] suggests a mean of 0.8 and a coefficient of variation of 0.1-0.2.

- $\Theta^{-1}_{c_{f,k,EC}}$: Davenport [56] suggests a mean of 0.9 and a coefficient of variation of 0.1-0.2. Measurements done by Svend Ole Hansen et al. [59] on a benchmark model of a

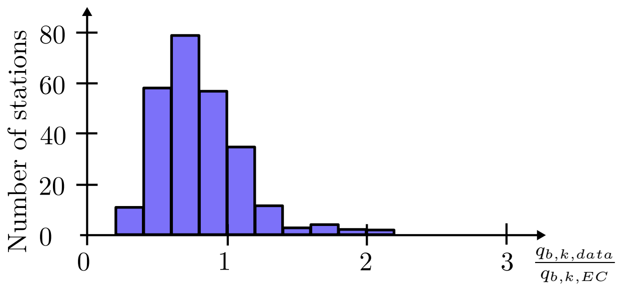

Figure 9: Histogram of the ratios of the characteristic values $q_{b,k,Data}$ obtained from data of the German Meteorological Service [57] and the characteristic values $q_{b,k,EC}$ of the respective location specified in the Eurocode [45].

tall building [60] confirmed these values with a tendency towards the upper bound.

- $\Theta^{-1}_{c_{sd,k,EC}}$: Davenport [56] suggests a mean of 1.0 and a coefficient of variation of 0.1-0.2.

C. Relative errors in the estimation of characteristic wind load model components according to advanced models

In the following we justify the distribution parameters of table 4. The advanced models are presumed to be the most accurate state-of-the-art models. Hence, no reference model serving as reference truth is available. Instead, measurement data must be evaluated in order to justify the parameters of the error distributions. We thereby follow the ISO/IEC guide [61]:

- $\Theta^{-1}_{q_{b,k,adv}}$: We assume that advanced wind load modeling techniques use on-site wind data to estimate the characteristic wind velocity pressure. We postulate that such an analysis leads to an unbiased estimator. Based on the data from the German Meteorological Service [57] described in Anex B, we estimate the coefficient of variation of $\Theta^{-1}_{q_{b,k,adv}}$ as 0.1. This estimate is based on the assumption that extreme wind pressures follow a Gumbel distribution.

- $\Theta^{-1}_{c_{e,k,adv}}$: We presume that advanced wind modeling techniques use on-site wind data to predict $c_e(z)$ [17, 62]. According to Eurocode 1 [45], the characteristic exposure coefficient is calculated as

$$c_e(z) = 0.19 \cdot \left(\frac{z_0}{0.05}\right)^{0.07} \cdot \ln\left(\frac{z}{z_0}\right) \tag{27}$$

  where z is the height above ground and z_0 is the roughness length of the terrain. Kelly and Jørgensen [63] determine the uncertainty in the prediction of z_0 using on-site data. They find that z_0 can be estimated with a coefficient of variation 5 %, given one year of on-site wind data. This leads to an uncertainty in the order of 2 % in the estimate of $c_e(z)$. Considering the inherent uncertainty of Eq. 27, we assume that the advanced modeling technique results in a coefficient of variation of 5 % on the $c_e(z)$ estimate.

- $\Theta^{-1}_{c_{f,k,adv}}$: We presume that advanced wind modeling techniques utilize wind tunnel tests to predict the force coefficient. Wind tunnels can be calibrated such that they lead to unbiased results [64]; hence $\mathrm{E}[\Theta^{-1}_{c_{f,k,adv}}] = 1$. The coefficient of variation of $\Theta^{-1}_{c_{f,k,adv}}$ is follows Long [65], who evaluates wind tunnel data of a simple rectangular building and compares it with results from the full scale test reported in [66, 67]. From the results of [65], we derive a coefficient of variation of $\Theta^{-1}_{c_{f,k,adv}}$ equal to 0.15. This choice is confirmed by Fritz et al. [68] who estimated the variability of wind effects based on tests conducted at six wind tunnel laboratories. Their results show that the coefficient of variation of the measured 50th percentiles of the peak force coefficients of a roof tap nearest a building corner is 0.19 on average. This values should be a bit lower, since Fritz et al. also included the roughness of the terrain.

- $\Theta^{-1}_{c_{sd,k,adv}}$: No data were found to estimate the distribution of the relative error in the estimation of the characteristic structural factor following advanced wind load modeling techniques. Because the estimation of the structural factor according to Eurocode is already unbiased, the estimation according to advanced wind load modeling techniques is also assumed to be unbiased. Hence $\mathrm{E}[\Theta^{-1}_{c_{sd,k,adv}}] = 1$. The coefficient of variation of $\Theta^{-1}_{c_{sd,k,adv}}$ is presumed to be 0.1.